JOURNAL OF CATALYSIS 155, 12–20 (1995)

Electrode Potential of a Dispersed Raney Nickel Electrode during Acetone Hydrogenation: Influence of the Solution and Reaction Kinetics

J. Pardillos-Guindet,*,[1] S. Vidal,* J. Court,* and P. Fouilloux†,[1]

*Labortatoire d'Etudes Dynamiques et Structurales de la Sélectivité (LEDSS 1), Université Joseph Fourier, B.P. 53, 38041 Grenoble Cédex, France; and †Unité Mixte CNRS-Rhône Poulenc, 24 Avenue Jean Jaurès, 69153 Décines-Charpieu Cédex, France

Received January 5, 1994; revised February 22, 1995

The hydrogenation of acetone was investigated in basic aqueous solutions with undoped and chromium-doped catalysts. The reaction was carried out under pressure in an autoclave equipped with a reference electrode. The consumption of hydrogen and the electrode potential were measured during the course of the reaction. A mathematical model was applied which fits the experimental kinetic data well. It allows the computation of the rate constant and the adsorption equilibrium constants. The kinetics obey a Langmuir–Hinshelwood mechanism with competitive adsorption. The metallic catalyst particles behave like a dispersed electrode and an electrochemical double layer is formed at their surface. In the presence of hydrogen alone, the metal potential obeys the Nernst law for the hydrogen electrode. During acetone hydrogenation, the double layer is modified and the measured potential goes to the positive region for several tens of millivolts, depending on whether the catalyst is doped or not. In all cases an experimental correlation was found between this experimental potential rise and the reaction rate.

INTRODUCTION

Raney nickel catalysts are extensively used in industry and research for hydrogenation, hydrogenolysis, oxidation, and cyclization reactions of different organic compounds. Moreover, Justi *et al.* (1) and Mund *et al.* (2) have also shown that Raney nickel is a suitable catalyst for fuel cell hydrogen electrodes. In the presence of water or polar solvent an electrochemical double layer (2, 3) is formed on the metallic surface, with H^+ adsorbed species being balanced by a negative charge on the metal. This metal charge is responsible for the Nernst potential of the hydrogen electrode. If an organic compound is introduced into this equilibrated system, the double layer is modified by its adsorption and the electrochemical potential is shifted because the surface sites, active in hydrogen dissociation, and the distribution of electrical charges are also modified.

The course of the hydrogenation of nitroaromatics on a skeletal nickel catalyst has been studied by parallel observation of the catalyst potential changes during hydrogenation (4–7). A connection between the liquid phase concentration of nitrobenzene, the electrode potential, and the reaction rate was found (5, 7). This connection allows the application of the measured potential to the investigation of the reaction kinetics and process control. In the hydrogenation of unsaturated compounds, Druz (8) has shown that a linear relationship must occur between the catalyst potential shift and the reaction rate, which makes it possible to determine specific characteristics of the catalyst. To go thoroughly into the interpretation of this type of data we thought it of interest to combine them with a complete kinetic study and that this problem should be revisited using a simple reaction, such as the hydrogenation of acetone dissolved in water.

The difficulty of ketone reduction by catalytic hydrogenation is in an intermediate position with respect to that of other unsaturated functional groups. De Ruiter and Jungers (9) and van Mechelen and Jungers (10) found that the reactivity decreases in proportion to the total number of alkyl carbon atoms for open chain ketones. That is why most authors have chosen the hydrogenation of acetone, which is the first member of the series, as a test reaction. Moreover, in moderately basic solutions this molecule does not give side reactions, such as condensations, and the evolution of the reaction can be followed very simply by measuring the hydrogen consumption, as described by Kishida and Teranishi (11), Kishida *et al.* (12), and Lemcoff (13).

The first kinetic study on the hydrogenation of liquid acetone on Raney nickel was made by Freund and Hulburt (14). They have shown that internal diffusion is rate controlling and the reaction order with respect to hydrogen is zero. Kishida and Teranishi (11) devoted a paper to the

[1] To whom correspondence should be addressed.

0021-9517/95 $12.00

particular case of acetone in various solvents. Their work consisted of a comparison between the rates in alcoholic solvents and in hydrocarbons. The kinetics were interpreted by a rate equation derived on the basis of the Langmuir–Hinshelwood mechanism and under the assumption that hydrogen, acetone, and solvent are adsorbed competitively on the catalyst surface. Moreover, Lemcoff (13) took into account the change in hydrogen solubility with the composition of the solution. The concentration of hydrogen was calculated from a correlation developed for mixtures of solvents.

The hydrogenation reaction of acetone dissolved in water must be considered apart from those carried out in organic solutions (11). The high dielectric constant of water and the fact that it is an electrolyte introduce a new parameter, namely, the pH of the solution.

In the present work, the hydrogenation of acetone was investigated in basic aqueous solutions with undoped and chromium-doped Raney nickel catalysts. The consumption of hydrogen at a constant pressure and the electrode potential of the metallic catalyst were simultaneously measured during the course of the reaction.

EXPERIMENTAL

Preparation and Characterization of Catalysts

The standard Raney nickel catalyst (RNi) was obtained by leaching a Ni–Al (50 : 50, w : w) commercial alloy (Prolabo) with a 6 mol · liter^{-1} boiling sodium hydroxide solution (15). Chromium-doped catalyst (RNi–xCr) was prepared according to the following procedure (16): portions of RNi, washed to neutrality, were impregnated with a chromium chloride ($CrCl_3 \cdot 6H_2O$, Merck) solution to give the desired chromium loading (x is the Cr/Ni atomic ratio).

The bulk compositions of the catalysts were determined by chemical analysis and all compositions were expressed as atomic ratios. The specific surface areas were obtained by means of low-temperature nitrogen physisorption and the metallic surface areas using adsorption of 3-methylthiophene in liquid phase in the presence of hydrogen (15). Table 1 reports the physical and chemical characteristics of the catalysts.

Hydrogenation Reaction Conditions

The activity and the electrochemical potential of the catalyst slurries were simultaneously measured in a specially designed 150-ml autoclave. Hydrogenation was carried out in a liquid phase in this autoclave under magnetic stirring (1250 rpm), at constant pressure (10^6–5×10^6 Pa) and temperature (310 K). Before use the catalyst was carefully washed with distilled water five times. The catalyst (0.2–0.5 g) and the sodium hydroxide solution (40 ml; pH 12.5) were loaded and the autoclave was flushed with hydrogen. The mixture was pretreated under hydrogen pressure at room temperature for 1 h. The temperature was stabilized at 310 K and distilled acetone (0.1–15 ml) was then injected. The introduction of acetone was considered to be the starting point of the hydrogenation reaction. Hydrogen consumption was determined by recording the pressure drop in a reservoir of known volume. In the range explored in our experiments, we verified that the initial rates were proportional to the weight of the catalyst, to ensure that we had no gas–liquid transfer limitations.

The catalyst metal particles suspended in the stirred slurry strike the stainless steel reactor wall and impart their electrochemical potential to it. To enable us to perform the potential measurements the autoclave contained a built-in Hg–HgO/KOH 1 M reference electrode.

RESULTS

Kinetics of Liquid Phase Hydrogenation of Acetone on a Raney Nickel Catalyst

1. Kinetics Experiments

The rate data obtained for the hydrogenation of acetone on updoped and chromium-doped Raney nickel catalysts in buffer solutions are shown in Fig. 1. The doped catalysts are much more active by a factor of 10 than the undoped ones. The activity is also strongly enhanced (Fig. 1a) for the two types of catalysts when the pH rises from neutrality to 12.5 and decreases above pH 12.5. In the aqueous phase, adsorption measurements were made by Fouilloux and Bussière by means of ^{14}C-labeled acetone

TABLE 1

Physical and Chemical Characteristics of Catalysts

Catalyst	Bulk composition (at.%)			Surface area ($m^2\ g^{-1}$)	
	Al/Ni	Cr/Ni	Fe/Ni	Total by BET	Metallic (Ni)
RNi	9.3	0	0.6	74	60
RNi–2.2Cr	9.4	2.2	1.1	96	63

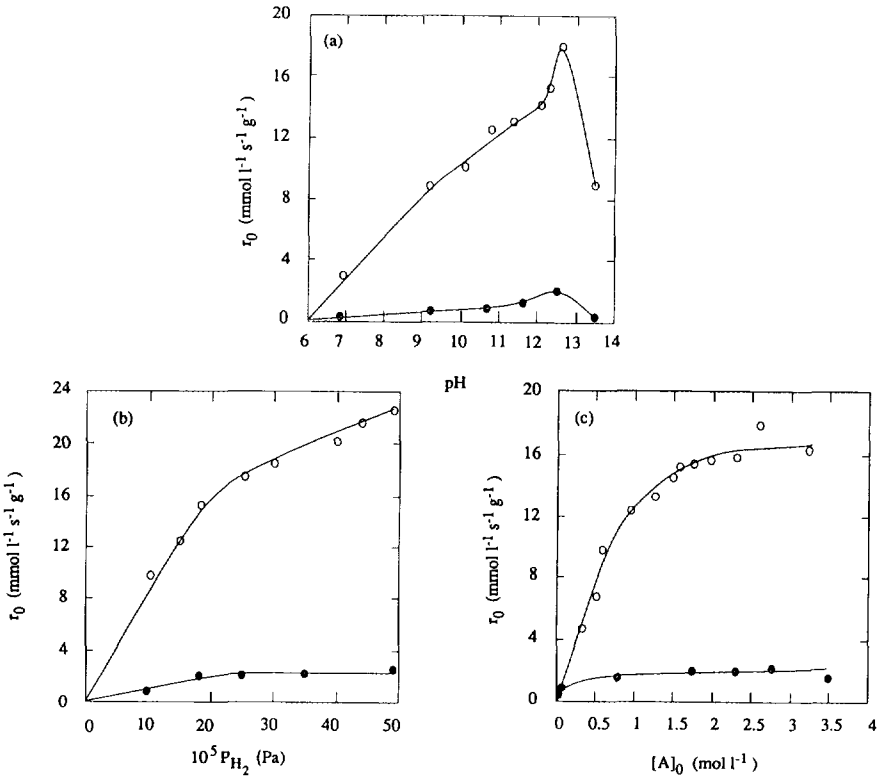

FIG. 1. Initial hydrogenation rate of acetone at 310 K. (a) Influence of pH; $[A_0] = 2.75$ mol · liter^{-1}; $P_{H_2} = 25 \times 10^5$ Pa. (b) Influence of hydrogen pressure, $[A_0] = 2.75$ mol · liter^{-1}, pH 12.5. (c) Influence of initial acetone concentration; $P_{H_2} = 25 \times 10^5$ Pa; pH 12.5. (○) RNi–2.2Cr; (●) RNi.

(17, 18). The results concerned only irreversibly adsorbed acetone and showed that the adsorption follows the Langmuir equation and that alkaline solutions favor the irreversible adsorption. Fouilloux and Bussière (17) give experimental evidence that the hydrogenation rate is proportional to the amount of irreversibly adsorbed acetone at all of the pH values. Our results are in good agreement with their observations.

The hydrogenation reaction of acetone was then performed in sodium hydroxide solution (pH 12.5) at 310 K, with on one hand the initial acetone concentration being varied from 0.03 to 3.7 mol · liter^{-1} under a constant hydrogen pressure and on the other hand the pressure being varied from 10^6 to 5×10^6 Pa for a constant acetone concentration of 2.75 mol · liter^{-1}. The results are reported in Figs. 1b and 1c. Under these conditions, the doping effect of chromium is still observed. The rate dependence on acetone concentration and hydrogen pressure is not linear. On the doped catalyst the specific rate increases rapidly to reach a plateau. On standard Raney nickel this maximum reaction rate is attained even more rapidly. This behavior suggests that a mathematical equation based on a Langmuir–Hinshelwood mechanism could be applied to the experimental data.

2. *Langmuir–Hinshelwood Rate Expression*

Organic species and hydrogen could be adsorbed competitively on the surface of the catalyst or noncompetitively on different sites. The rate equations are determined with the following assumptions:

—the adsorption equilibria are maintained during the reaction;

—the overall rate of hydrogenation is governed by the rate of chemical reaction on the surface;

—the elementary reactions are first order with respect to the surface concentration of acetone;

—the hydrogen adsorption is dissociative.

2.1 *Noncompetitive adsorption (N.C.A.).*

$$-\frac{d[A]}{dt} = \frac{kb_A[A]\sqrt{b_{H_2}P_{H_2}}}{(1 + \sqrt{b_{H_2}P_{H_2}})(1 + b_A[A] + b_I[I] + b_S[S])}, \quad [1]$$

where b_X is the adsorption equilibrium constant of X, $[X]$ is the concentration of the component X in the liquid phase, A is the acetone, I is the isopropanol, and S is the solvent.

Since the hydrogen pressure is maintained constant during the course of the reaction, expression (1) gives

$$-\frac{d[A]}{dt} = \frac{[A]}{(\alpha + \beta[A])} \quad [2]$$

with

$$\alpha = \frac{(1 + \sqrt{b_{H_2}P_{H_2}})(1 + b_I[A]_0 + b_S[S])}{kb_A\sqrt{b_{H_2}P_{H_2}}} \quad [3]$$

and

$$\beta = \frac{(1 + \sqrt{b_{H_2}P_{H_2}})(b_A - b_I)}{kb_A\sqrt{b_{H_2}P_{H_2}}} \quad [4]$$

From Eq. (2) separation of variables and integration lead to

$$t = \alpha \ln\left(\frac{[A]_0}{[A]}\right) + \beta\{[A]_0 - [A]\}. \quad [5]$$

2.1. Competitive adsorption (C.A.)

$$-\frac{d[A]}{dt} = \frac{kb_A[A]\sqrt{b_{H_2}P_{H_2}}}{(1 + \sqrt{b_{H_2}P_{H_2}} + b_A[A] + b_I[I] + b_S[S])^2} \quad [6]$$

The rate expression [6] can be rewritten in a more simplified manner by means of two new parameters

$$-\frac{d[A]}{dt} = \frac{[A]}{(\delta + 2\sqrt{2\delta\gamma}[A] + 2\gamma[A]^2)} \quad [7]$$

defined as

$$\delta = \frac{(1 + \sqrt{b_{H_2}P_{H_2}} + b_I[A]_0 + b_S[S])}{kb_A\sqrt{b_{H_2}P_{H_2}}} \quad [8]$$

and

$$\gamma = \frac{(b_A - b_I)^2}{2kb_A\sqrt{b_{H_2}P_{H_2}}}. \quad [9]$$

After integration of Eq. [7] the new expression is

$$t = \delta \ln\left(\frac{[A]_0}{[A]}\right) + 2\sqrt{2d\gamma}([A]_0 - [A]) + \gamma([A]_0^2 - [A]^2). \quad [10]$$

3. Computation of the Kinetic and Adsorption Constants

Equations [5] and [10] depend on two parameters: these are α, β when adsorption is noncompetitive and δ, γ when adsorption is competitive. The computation using the SIMPLEX algorithm (19) of these two pairs of parameters has been tentatively made. It is actually possible to adjust the two sets α, β, and δ, γ to the experimental points and to put them in Eqs. [5] and [10]: the recalculated kinetic curves fit the experimental points equally well (Fig. 2). Hence at this stage it is not possible to settle the question of the competitiveness or noncompetitiveness of the adsorption. Nevertheless, the kinetic parameters are estimated from the above variations and the results are summarized in Table 2.

The fractional surface coverages of acetone (θ_A) and hydrogen (θ_H) were also computed using the adsorption equilibrium constant values. Based on the assumption of a noncompetitive adsorption, Figs. 3a and 3b show that the acetone coverage is already high at low concentration and hydrogen coverage is low and constant even at high

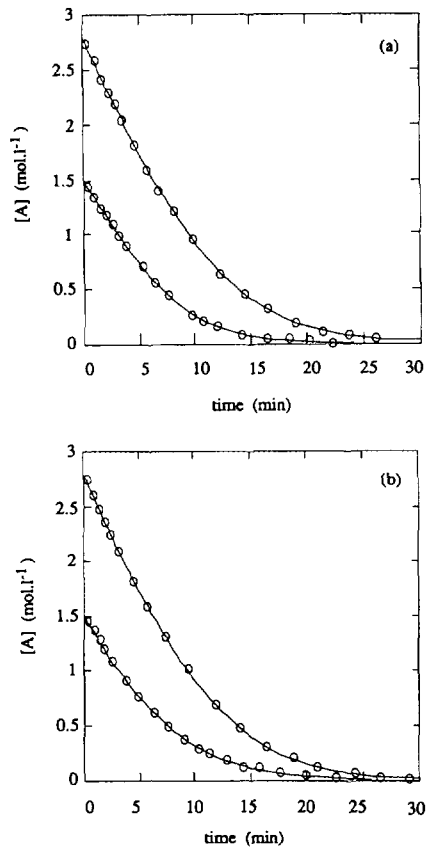

FIG. 2. Hydrogenation of acetone over RNi–2.2Cr at 310 K: experimental points (O) and computed curve (—) for acetone concentration as a function of time. (a) Competitive adsorption (C.A.). (b) Noncompetitive adsorption (N.C.A.). $P_{H_2} = 25 \times 10^5$ Pa; $[A_0] = 2.75$ mol · liter^{-1}.

TABLE 2

Adsorption Equilibrium Constants and Rate Constants

Catalyst	b_A(liter · mol^{-1})	b_I(liter · mol^{-1})	$10^5 \cdot b_{H_2}$(Pa^{-1})	k(mol · liter^{-1} · s^{-1} · g^{-1})
RNi				
N.C.A.	4.6	0.3	5×10^{-3}	0.01
C.A.	4.5	2.0	1.3	0.02
RNi–2.2Cr				
N.C.A.	1.0	0.3	10^{-3}	0.12
C.A.	1.5	0.4	0.1	0.15

Note. N.C.A.: noncompetivie adsorption; C.A.: competitive adsorption.

acetone concentration. For the opposite situation where the hypothesis of competitive adsorption is made, we can see in Figs. 3c and 3d that the computation gives decreasing θ_H and increasing θ_A for rising acetone concentrations. In the two cases, doped and undoped Raney nickel behave in a very similar manner. However, it seems that a θ_H value comprised between 0.15 and 0.25 in the case of noncompetitive adsorption is not realistic, Raney nickel being well known to take up large amounts of hydrogen. The values computed in the hypothesis of competitive adsorption and comprised between 0.25 and 0.8 are much more realistic. This gives some evidence in favor of competitive adsorption.

Chromium addition to the catalyst increases the initial hydrogenation rate (Fig. 1), which is proportional to the fractional surface coverages. θ_A and θ_H variations versus $[A]_0$ are almost similar for RNi and RNi–2.2Cr. The promotion of the activity by a factor α 10, resulting from chromium doping, is due to the increase in the rate constant rather than to the adsorption constants.

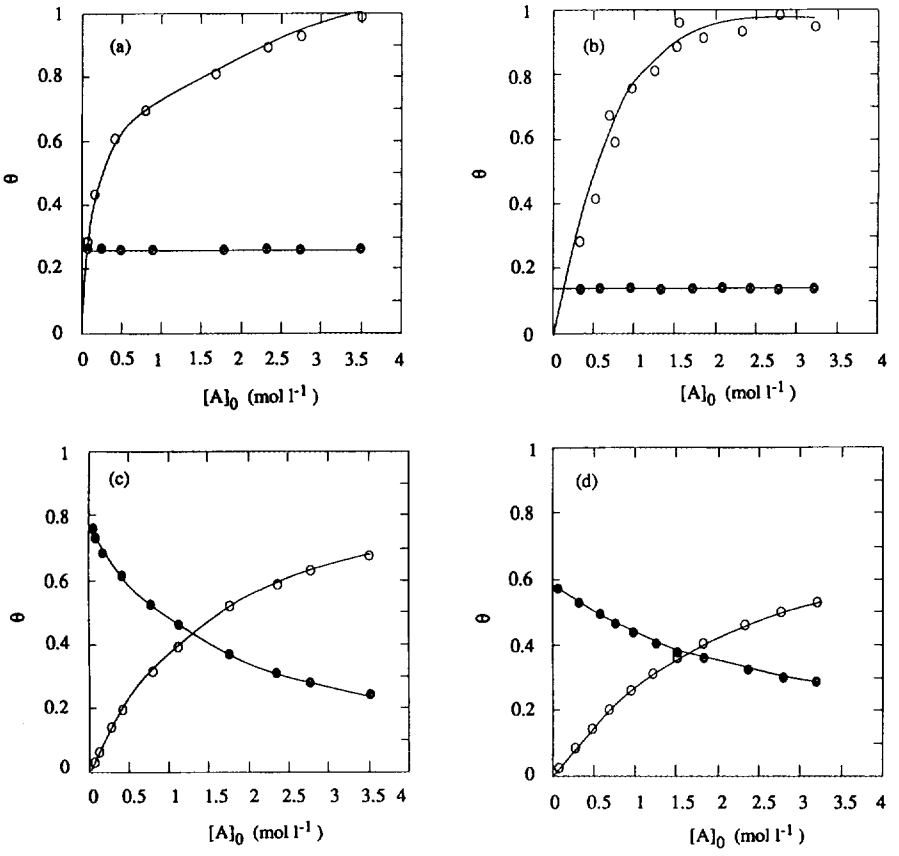

FIG. 3. Fractional surface coverages of acetone (○) and hydrogen (●) versus $\sqrt{[A_0]}$ at 310 K with $P_{H_2} = 25 \times 10^5$ Pa. (a) N.C.A. for RNi. (b) N.C.A. for RNi–2.2Cr. (c) C.A. for RNi. (d) C.A. for RNi–2.2Cr.

TABLE 3

Influence of Hydrogen Pressure, Temperature, and pH of Electrolyte Solution of the Measured Raney Nickel Potential

Catalyst potential (mV/SCE)	Parameters									
	Pressure[a] (10^5 Pa)		Temperature[b] (°K)		pH[c]					
	1	50	293	310	6.9	9.2	10	10.9	12.5	13.5
$E_{(Nernst)}$	−1014	−1066	−985	−1005	−690	−830	−884	−920	−1005	−1085
$E_{(measured)}$	−1010	−1057	−990	−1000	−730	−810	−894	−924	−1000	−1087

[a] pH 12.5; T = 310 K.
[b] pH 12.5; $P_{H_2} = 25 \times 10^5$ Pa.
[c] T = 310 K; $P_{H_2} = 25 \times 10^5$ Pa.

Electrochemical Potential of Raney Nickel Catalysts

1. Conditions of Catalyst Potential Measurements

Sokolsky and Chmonina (4) claimed that a catalyst metallic powder, under very intense stirring in acid, neutral, and alkaline aqueous solutions, is able to communicate its own potential to a gold or platinum electrode. A large amount of powder is used in this technique. To confirm that we were able to carry out this measurement under hydrogen pressure, we verified that the potential of a compact fuel cell electrode made of bound Raney nickel particles, having a good electrical contact with the measuring electrode, is the same under our conditions as the potential of the autoclave wall bombarded by the metallic particles in suspension. Thus they impose their potential due to their high surface area. Without a catalyst the potential is nonreproducible and unstable probably because the oxides on the surface of 316 stainless steel are not stable under the conditions of the experiments.

Following the Nernst equation, the potential of a hydrogen electrode is shifted by 58 mV for a pH variation of one unit. To avoid a parasitic potential shift, we checked this parameter from time to time during the experiments.

2. Electrode Potential under Hydrogen Pressure without Reaction

Under equilibrium conditions, the metallic catalyst (undoped and doped Raney nickel) placed into the aqueous solution and under hydrogen gives rise to the following reaction:

$$H_2 \rightleftharpoons 2H_{ads} \rightleftharpoons 2H^+ + 2e^-.$$

Every catalyst grain behaves like a reversible hydrogen electrode and its potential follows the Nernst law:

$$E_{V/NHE} = \frac{RT}{F} \ln \frac{[H^+]}{\sqrt{P_{H_2}}}. \qquad [11]$$

We verified that the measured Raney nickel potential depends only on the temperature, the hydrogen pressure, and the pH of the aqueous solution. The comparison between the expected values and the measured data is summarized in Table 3.

3. Electrode Potential in the Presence of Acetone

A typical change in the potential of the Raney catalysts during hydrogenation is reported in Fig. 4. During the first part of the experiment, represented by the segment AB of the curve, the reactor contains only hydrogen, catalyst, and solvent. The potential value of the catalyst is in agreement with the Nernst law. At point B, acetone is introduced into the reactor. The catalyst potential undergoes immediately an anodic shift ΔE_0 of several tens of millivolts to point C. At the same time hydrogen is consumed and the potential starts shifting toward the cathodic region, following the curve segment CD.

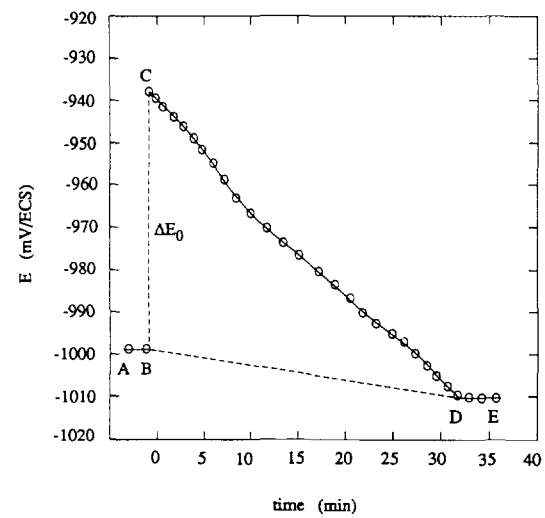

FIG. 4. Potential of the Raney nickel catalyst during the hydrogenation of acetone on RNi–2.2Cr at 310 K; $P_{H_2} = 25 \times 10^5$ Pa; $[A_0] = 2.75$ mol · liter^{-1}.

TABLE 4

Influence of Isopropanol on the Raney Nickel Electrode Potential (T = 310 K; P_{H_2} = 25 × 10^5 Pa)

Isopropanol (wt% in solution)	0	4	13	20	32	40	53	60
pH	9.2	9.3	9.6	9.9	10.1	10.3	10.5	10.7
$\Delta E_{expected}$(mV)	0	−4	−22	−39	−48	−60	−78	−85
$\Delta E_{expected}$(mV)	0	−4	−17	−30	−46	−58	−68	−81

The value of the reversible hydrogen potential on segment DE when hydrogenation is finished is slightly more cathodic than on AB. That is why, with isopropanol being the product of the reaction, its influence on the catalyst potential must be checked. The result of isopropanol addition to a water alkaline solution is an increase in the pH value. Table 4 shows that the cathodic shift with reference to the initial potential without isopropanol is only due to the modifications of the pH. This can be explained from the Nernst law and accounts for the difference between AB and CE.

The most important fact observed in Fig. 5 is that the potential shifts are three times greater for the undoped than for the chromium-doped catalyst. This situation prevails whatever the pH, the hydrogen pressure, and the initial acetone concentration are, although the doping induces 10 times enhancement of activity.

The initial catalyst potential shifts ΔE_0, measured when acetone is hydrogenated on doped and undoped Raney nickel catalysts in buffer solutions, are reported in Fig. 5a. Figure 5b shows that ΔE_0 is slightly dependent on hydrogen pressure. Figure 5c illustrates a Langmiur-like dependence of the initial potential shift on acetone initial concentration. This suggests that the ΔE_0 values taken

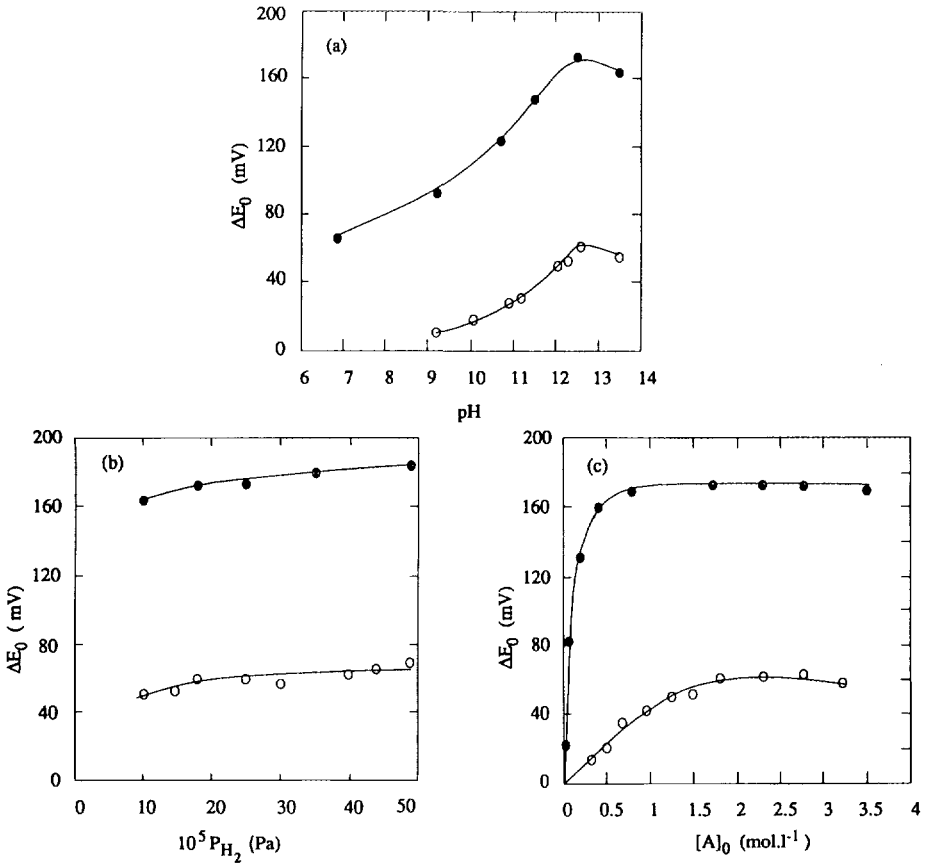

FIG. 5. Catalyst potential shift ΔE_0 during the hydrogenation of acetone at 310 K. (a) Influence of pH; $[A_0]$ = 2.75 mol · liter^{-1}; P_{H_2} = 25 × 10^5 Pa. (b) Influence of hydrogen pressure; $[A_0]$ = 2.75 mol l^{-1}; pH = 12.5. (c) Influence of initial acetone concentration; P_{H_2} = 25 × 10^5 Pa; pH 12.5. (○) RNi–2.2Cr; (●) RNi.

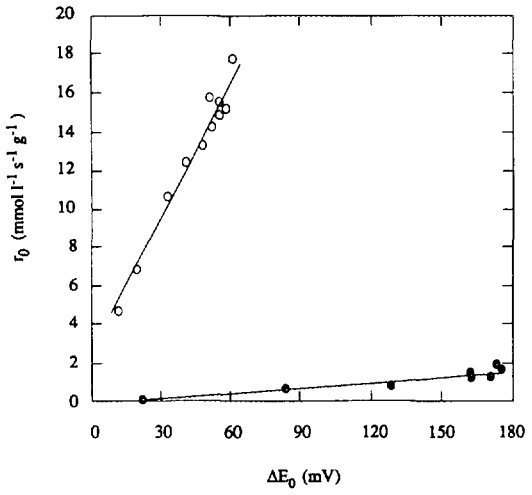

FIG. 6. Initial rate as a function of the catalyst potential shift ΔE_0 at 310 K with $P_{H_2} = 25 \times 10^5$ Pa and pH 12.5. (○) RNi-2.2Cr; (●) RNi.

by the catalysts for different acetone concentrations could vary linearly with the initial hydrogenation rates (20), which is confirmed by Fig. 6. From the above kinetic data and since these rates are proportional to the acetone adsorption, ΔE_0 should be proportional to θ_A. This statement is borne out (Fig. 7) whatever the hypothesis made to calculate the acetone coverage. However, for the undoped Raney nickel, a small part of the curve is linear and after that ΔE_0 is independent of θ_A. The electrochemical potential reveals a difference between the two catalysts: for the doped Raney, ΔE_0 is proportional to θ_A over all the experimental range, which is not the case without doping.

DISCUSSION

The doped Raney nickel is at least 10 times more active in acetone hydrogenation than the undoped catalyst. If the pH of the solvent is increased from neutral to a value of 12.5, the enhancement in activity is much more pronounced for the doped catalyst: a synergetic effect takes place between the dopant and the basicity of the solution. Beyond this value, the basicity has a negative effect on activity. Hence the promotion of the activity for the hydrogenation of acetone by a base goes through an optimum.

The hydrogenation kinetics obey a Langmuir–Hinshelwood mechanism where acetone and hydrogen are adsorbed. The computation of the kinetic parameters based on this assumption gives curves which fit the experimental results well, for both competitive and noncompetive adsorption. However, the hydrogen coverages calculated for the first hypothesis are more consistent with a surface widely covered with hydrogen, as is commonly assumed for Raney nickel, giving evidence for a competitive mechanism as already shown by other authors (11, 13).

The electrochemical potential of the catalyst metallic particles is governed by the Nernst law under hydrogen pressure. At constant pH, when the hydrogenation takes place, the potential undergoes an anodic shift and comes back to a baseline when the reaction is finished. From a practical point of view, the potential is a probe for the end point of the hydrogenation, which could be very useful for process control.

From a theoretical point of view, several explanations can be considered to account for the potential variation during the hydrogenation reaction. First, we can consider that the electrode potential is only sensitive to hydrogen concentration and it is not modified by the presence of reactants, with the only effect of the hydrogenation reaction being to modify the local hydrogen pressure at the level of the sites. If this was true, the doped catalyst, which is 10 times more active than the standard one, would cause a higher depletion in hydrogen pressure due to transfer, i.e., a larger value of ΔE_0. It is the opposite situation that is observed, since the doped catalyst gives a smaller ΔE_0 (60 mV compared to 170 mV). Moreover, such cathodic shifts should correspond to very low hydro-

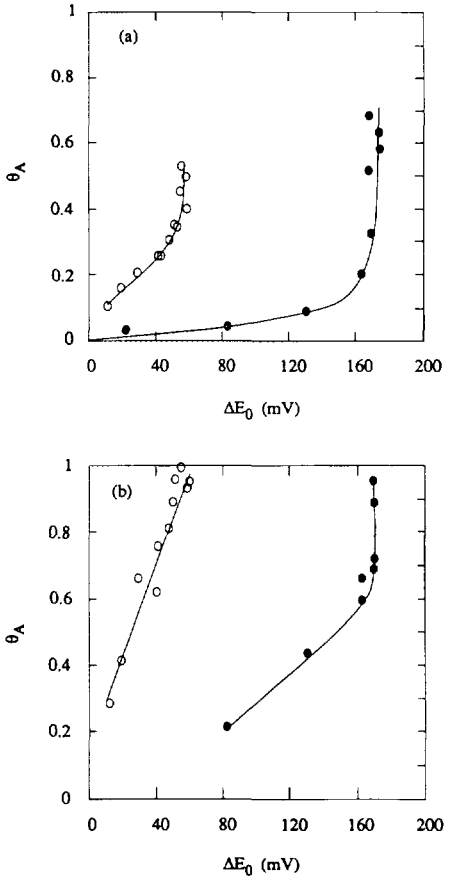

FIG. 7. Fractional surface coverage of acetone versus the catalyst potential shift ΔE_0 at 310 K with $P_{H_2} = 25 \times 10^5$ Pa and pH 12.5; (a) C.A. (b) N.C.A. (○) RNi-2.2Cr; (●) RNi.

gen virtual pressures and consequently to very low surface coverages, which is not the case. However, it is not impossible that hydrogen transfer could take a minor part in the potential shift.

A second mechanism to explain the catalytic hydrogenation in the basic solution (20) can be imagined. On one site we would have

$$H_2 + 2OH^- \rightleftharpoons 2H_2O + 2e^-$$

and on the next site

$$CH_3\text{–}CO\text{–}CH_3 + 2H_2O + 2e^- \rightleftharpoons CH_3\text{–}CHOH\text{–}CH_3 + 2OH^-.$$

Under this assumption, the role of hydrogen is only to produce electrons which are transferred through the metal to electrochemically reduce acetone to isopropanol and regenerate OH^- ions. After correction of the contribution of the pressure, the acetone reduction potential is 170 mV (130 + 40 mV) higher than the hydrogen electrode potential (21) and the maximum shift ΔE_0 is actually in this range. Thus, during hydrogenation, we would have a mixed potential comprised between the hydrogen electrode potential and the reduction potential of acetone. Moreover, this electrocatalytic mechanism would give theoretical support to the observed promoting effect of the base dissolved in the solvent. However, the electron flux needed to produce the observed hydrogenation rate would be very high and such an electrochemical reaction would probability give way to an overpotential higher than the observed ΔE_0 and therefore such a mechanism might only partially contribute to the isopropanol production. Even if this is not the chief route of the hydrogenation, it can accompany the reaction and serve as a probe proportional to acetone coverage on the surface. This linearity is verified on Fig. 7 for the doped catalyst and in the first part of the curve for standard Raney nickel. In this last case, in the second section, the potential is independent of adsorption at higher coverage. This can be explained by a second species of inactive adsorbed molecules.

Finally, a third explanation can be proposed: the acetone adsorption would induce a change in the surface double layer and the electronic distribution and therefore would modify the potential of the catalyst.

To sum up the discussion, the second hypothesis, based on a mixed potential acting at least as a probe reaction on adsorbed acetone, is the most attractive. If we go further and consider it as the chief reaction pathway, we can explain the mechanism of the base promoting effect. In any case the potential of the metallic catalyst joined to the hydrogenation kinetics study is a very useful tool to approach the reaction mechanism.

REFERENCES

1. Justi, E., Scheibe, W., and Winsel, A., German Patent 1019361, 1954.
2. Mund, K., Ritchter, G., and Sturm, F., *J. Electrochem. Soc. Electrochem. Sci. Technol.* **124,** 1 (1977).
3. Candy, J. P., Fouilloux, P., Keddam, M., and Takenouti, H., *Electrochim. Acta* **27,** 1585 (1982).
4. Sokolsky, D. V., and Chmonina, V. P., "Actes du II Congrès International de Catalyse," p. 2733. Technip, Paris, 1961.
5. Finkelshtein, A. V., and Anisimov, L. N., *Kinet. Katal.* **20,** 208 (1987).
6. Baumeister, P., Blaser, H. U., and Scherrer, W., "Heterogeneous Catalysis and Fine Chemicals II," Vol. 59, p. 321. Elsevier, Amsterdam, 1991.
7. Geike, R., Alscher, G., Kinza, H., and Turek, F., *Chem. Technol.* **41,** 301 (1989).
8. Druz, V. A., *Kinet. Katal.* **8,** 344 (1967).
9. De Ruiter, E., and Jungers, J. C., *Bull. Soc. Chim. Belg.* **58,** 210 (1949).
10. van Mechelen, C., and Jungers, J. C., *Bull. Soc. Chim. Belg.* **59,** 597 (1950).
11. Kishida, S., and Teranishi, S., *J. Catal.* **12,** 90 (1969).
12. Kishida, S., Murakami, Y., Imanaka, T., and Teranishi, S., *J. Catal.* **12,** 97 (1969).
13. Lemcoff, N. O., *J. Catal.* **46,** 356 (1977).
14. Freund, T., and Hulburt, H. M., *J. Phys. Chem.* **61,** 909 (1957).
15. Sane, S., Bonnier, J. M., Damon, J. P., and Masson, J., *Appl. Catal.* **9,** 69 (1984).
16. Hamar-Thibault, S., Masson, J., Fouilloux, P., and Court, J., *Appl. Catal.* **99,** 131 (1993).
17. Fouilloux, P., and Bussièere, P., *Journal de Chimie Physique* **70,** 1330 (1973).
18. Foulloux, P., *Appl. Catal.* **8,** 1 (1983).
19. Cacecu, M. S., and Cachevis, W. P., *Byte,* 340 (1984).
20. Finkel'stein, A. V., Morozova, M. I., Kuz'mina, Z. M., and Tarbeeva, N. A., *Kinet. Katal.* **28,** 210 (1987).
21. Bard, A. J., and Lund, H., Encyclopedia of Electrochemistry of the Elements, Organic Section, Vol. XII, p. 6, (A. J. Bard, Ed.) Dekker, New York, 1973.